Energy & Environmental Science

Accepted Manuscript

ROYAL SOCIETY OF CHEMISTRY

www.rsc.org/ees

Table of Contents:

- Colour graphic (8cmx 4cm)
- Text highlighting novely of work

Broader context (200 words)

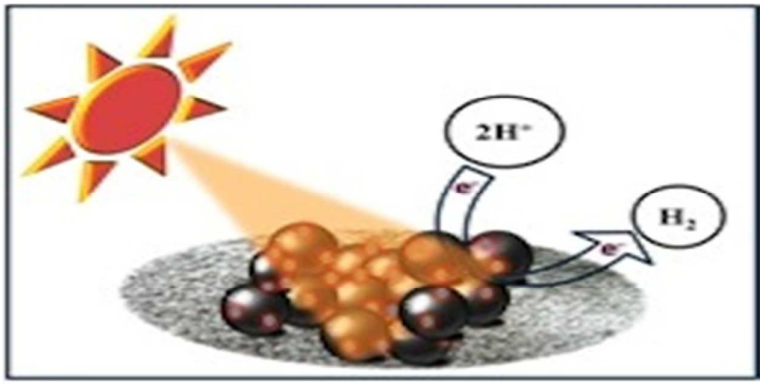

Platinized carbon nanostructured composite for photo catalytic hydrogen generation: synergism of carbon and platinum in nano form.

Broader Context:

Solar energy can be the answer to the questions raised on fulfilling the world's energy demands, subject to its efficient utilization. The solar energy conversion to hydrogen mediated through photocatalytic splitting of water appears to be an ambitious yet positive step in this pursuit. Decades of extensive research in this regard have enriched the database on the various materials explored so far. The focus has now shifted towards carbon based nano materials, which are well known for their excellent light absorption and charge transfer properties. The carbon nanostructures, either singly or in combination with other semiconducting materials are expected to enhance hydrogen generation by virtue of their photothermal effect. They also facilitate the effective dispersion of metal nanoparticles. This research article is an attempt to

exploit the synergistic effect of both carbon and platinum in their nano form by exploiting their photothermal and plasmonic properties, respectively.

Journal Name

RSCPublishing

ARTICLE

Throwing light on Platinized Carbon nanostructured composite for hydrogen generation

Cite this: DOI: 10.1039/x0xx00000x

Priti A. Mangrulkar [a,b], Abhay V. Kotkondawar [a,b], Sumanta Mukherjee [c], Meenal V. Joshi [a,b], Nitin Labhsetwar [a,b], D.D. Sarma [a,c]* and Sadhana S. Rayalu [a,b]*

Received 00th January 2012,
Accepted 00th January 2012

DOI: 10.1039/x0xx00000x

www.rsc.org/

In the present study, we have synthesised carbon nanoparticles (CNPs) through a relatively simple (non-tedious) process using a hydrocarbon precursor. These synthesised CNPs in the form of elongated spherules and/or agglomerates of 30-55nm were further used as a support to anchor platinum nanoparticles. The broad light absorption (300-700 nm) and a facile charge transfer property of CNPs in addition to the plasmonic property of Pt make these platinized carbon nanostructures (CNPs/Pt) a promising candidate in photocatalytic water splitting. The photocatalytic activity was evaluated using ethanol as the sacrificial donor. The photocatalyst has shown remarkable activity for hydrogen production under UV-visible light while retaining its stability for nearly 70h. The broadband absorption of CNPs, along with Surface Plasmon Resonance (SPR) effect of PtNPs singly and in composites has pronounced influence on the photocatalytic activity, which has not been explored earlier. The steady rate of hydrogen was observed to be 20 $\mu molh^{-1}$ with exceptional cumulative hydrogen yield of 32.16 mmol $h^{-1}g^{-1}$ was observed for CNPs/Pt, which is significantly high for that reported for carbon based systems.

Introduction

Harvesting solar energy for its effective conversion into a chemical fuel carrier like hydrogen continues to intrigue researchers worldwide. From the viewpoint of efficient solar energy conversion, the pre-requisite being visible light activity, high quantum efficiency and long term stability of the photo catalyst. In this context, recent research scenario is driven towards the quest for new and advanced materials, and it is largely centered on nano-structured materials. This is essentially because the particle size of the materials when scaled down, can lead to exciting changes in their properties, consequently making way for their application in various fields. Amongst several nanostructured materials that are being reported for various applications, carbon based nano materials have created their niche.

The different allotropes of carbon namely- graphite, graphene, carbon nanotubes, fullerenes have found use in many applications such as catalyst support[1,2], adsorbents [3,4], batteries [5], transistors[6], diodes[7], sensors [8,9] etc. The sp^2-hybridized state of elemental carbon possesses structural variations that can range from being amorphous to being highly crystalline. After the discovery of C60 molecule and other fullerenes [10] followed by carbon nano tubes by Ijima in 1991[11], the field has generated interest and has witnessed considerable growth. Belonging to this rich family of carbonaceous materials, carbon nano particle (CNP) is an important member.

There are several routes both physical as well as chemical by which these CNPs may be synthesized. Physical routes include laser ablation of graphite or high radiation based creation of point defects in diamonds. On the other hand, chemical routes include processes like carbonization of carbohydrates, thermal decomposition of small molecules, pyrolysis of polymers etc.

These carbon nanoparticles are usually formed as a result of incomplete combustion of either liquid or gaseous hydrocarbons. They are non-fluorescent, hydrophobic particles with size ranging typically from 20-800 nm. On further purification and functionalization, these particles may become

hydrophilic and also exhibit fluorescence[12]. Although, the fluorescent CNPs have been widely exploited for bio imaging and sensing applications, the non-fluorescent particles have been poorly explored.

Literature investigating the role of carbon-based nanostructures in the field of photo catalysis is available. In most of these reports, carbon nanostructures have been used in conjunction with a semiconductor like TiO_2, CdS, Fe_2O_3 etc. In these photo catalytic systems, their role in the photo catalytic reaction has been observed to be varied ranging from being a sensitizer, a support or even a co-catalyst [13-19]. Recently, Akimoto *et al.* demonstrated the generation of hydrogen by charcoal powder by laser irradiation[20]. They concluded that the carbon powder acted as a sacrificial agent in the photoreaction. Irrespective of the role of carbon nanostructures in a photocatalytic reaction, they are known to enhance it significantly which may be because of several reasons. 1) They suppress the electron-hole recombination reaction and aid in efficient shuttling of electrons. 2) They can act as sensitizers by harvesting light and even leading to extension of the absorption maxima by forming chemical bonds when present with semi conductors. 3) Owing to their hydrophobicity, they can help in uniform adsorption of organic substrates (or organic donors) thereby facilitating the reaction. 4) As a support, they can help in efficient dispersion of semiconductors as well as metal nanoparticles. 5) The most striking feature of carbon nanostructures is their ability to absorb electromagnetic radiation particularly in the infrared region. This absorption of light leads to generation of significant amount of heat in addition to the induction of phonon resonances[21]. Carbon nanostructures can thus either singly or in combination with other semiconducting materials are expected to enhance hydrogen generation by virtue of their photo thermal effect.

All the aforementioned factors in addition to the relatively inexpensive nature of carbon nanomaterials make them attractive candidates in photocatalysis. Recently, a report stated that in contrast to the graphitic phase, carbon nanostructures exhibit metallic or semiconductor properties, which make them useful in the field of catalysis as they aid in the charge, transfer process[22]. Exploring along these lines, in our present investigation, we have synthesized non-fluorescent carbon nanostructures through the combustion of a hydrocarbon precursor (vegetable oil). The synthesis procedure is relatively simple and green. Furthermore, these carbon nanostructures were loaded with platinum nanoparticles *via* a photodeposition method. The photodeposition route ensures high deposition of the noble metal and also eliminates the calcination step. The resulting platinized carbon nanostructured composite was evaluated in photo catalytic water splitting reaction, using ethanol as the sacrificial donor.

Experimental

Materials and Method

The hydrocarbon (Soybean oil) used as precursors was purchased from local market and was used without further purification. Chloro platinic acid ($H_2PtCl_6.6H_2O$) and ethanol were procured from E-Merck, India Ltd.

Synthesis of CNPs

CNPs were synthesized by bringing about the combustion of hydrocarbon precursor (Soybean oil). In a typical procedure, the precursor for CNPs was taken in a container and cotton wick was completely immersed in it. When the cotton wick soaked with the oil was burned, the hydrocarbons made up of hydrogen and carbon combine with oxygen to form water and carbon dioxide. The hydrogen burns more quickly than the carbon so there is an area of the wick, which is carbon rich. A brass plate was kept close to the wick and the soot particles typically of 30-55 nm sizes were collected on the brass plate.

Photo deposition of Pt on CNPs:

Platinized carbon composite was formed by photodeposition of platinum nanoparticles onto CNPs. This takes place simultaneously during the course of the photocatalytic reaction in the presence of ethanol and water. The $PtCl_4^-$ ions get reduced to Pt, which was substantiated by XPS analysis.

Characterization

X-ray photoelectron spectroscopy measurements were performed on VSW spectrometer at a pressure $< 1\times 10^{-9}$ torr with Al Kα X-ray source (photon energy 1486.6 eV) at a pass energy of 20eV. Transmission electron microscopy (TEM) measurements were performed on Technai T-20 operated at an accelerating voltage of 200 kV. Photocatalysts in powdered formed were dispersed in ethanol and sonicated in an ultrasound bath for 15 min. A few drops of this suspension were then cast on a carbon coated cu grid. The samples were dried under vacuum overnight before analysis. The amount of Pt loaded onto the CNPs was estimated by ICP-MS (Perkin Elmer NexIon 300) operating at RF power of 1550 W and with plasma and carrier gas flow rates of 15.0 L/min and 1.2 L/min, respectively. Calibration was performed through standard solutions with the calibration coefficient of 0.9998. Samples were analysed after a suitable dilution with deionized water (Milli Q 18.0 Ω). CHNS analysis was carried out on Variol EL III CHNS.

Photocatalytic hydrogen production
Offline evaluations

The photo catalytic activity was evaluated for hydrogen production through offline evaluations. A stock solution of 0.1 mg mL^{-1} of CNPs was prepared by dispersing 1 mg of synthesized CNPs in 10 mL of ethanol and further sonicating it for 20 min. Aliquots from this solution were then taken depending upon the amount of catalyst desired in a photocatalytic reaction. In a typical experiment, a known amount of photocatalyst was taken in 20 mL borosilicate vial containing 10 mL of water. Ethanol was added as a sacrificial donor.

A known amount of Pt precursor solution was added to it. The vial was properly sealed and evacuated. The reaction mixture was then illuminated using two tungsten filament lamps of 200W each for 2h. The evolved gas was analysed on a gas chromatograph through manual injections. Hydrogen evolved was estimated through a standard calibration curve.

Online evaluations

The photocatalytic experiments were carried out in a borosilicate glass reactor (750 mL) with an inner irradiation reaction cell under ambient temperature (25 ^{0}C). A 400 W high-pressure mercury lamp was used as an illumination source. The IR fraction of the illumination source was filtered as a result of the cold water circulating through the illumination well. In a typical photo catalytic experiment for hydrogen production, 6 mL stock solution of the carbon nanoparticles (0.1 mg mL^{-1}) were dispersed in an aqueous solution (300 mL) containing ethanol (5%) as the sacrificial donor. A known amount of Pt was added to it. The photoreactor was completely covered by Aluminium foil to avoid losses due to light scattering. Prior to the exposure to the light, the reaction mixture was thoroughly evacuated by purging nitrogen, ensuring the complete removal of oxygen. After regular intervals (2h), the amount of hydrogen generated was evaluated through automatic gas sampling valve of a gas chromatograph equipped with TCD and 5A molecular sieve column.

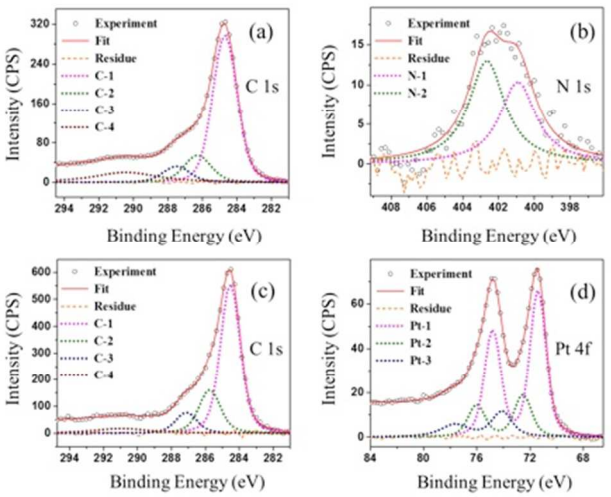

Fig.1 C 1s (a) and N 1s (b) X-ray photoelectron spectra obtained from the as synthesized CNPs sample. Fig 1c and 1d shows the XPS spectra obtained for C 1s and Pt 4f from the CNPs/Pt sample. In all the figures black open circles represents the experimental spectra. Various component spectra obtained from the decomposition of the experimental spectra are shown as magenta, green and blue and wine dotted line. The red solid lines are the overall fit whereas orange lines show the residues of such fits.

Results and Discussion

Characterization

x-ray photoelectron spectroscopy (XPS) was used to characterize chemical compositions of the as synthesized and Pt loaded CNPs. XPS spectra collected for C 1s and N 1s from CNPs are shown in Fig.1a and Fig 1b, respectively. We decompose these spectra to characterize different constituents present in the sample. Decomposition of the C 1s spectra obtained from CNPs shows presence of four different components. The C-1 component spectrum with a binding energy (BE) of 284.7 eV is associated with aliphatic and aromatic C, i.e. C with no N or O species in the surroundings, present in the CNP sample [23,24,25]. The components C-2 and C-3 with BEs of 286.3 eV and 287.6 eV are associated with C-O 25 (and C=N 23) and C=O 25 kinds of species present at the surface of the CNPs. The higher BE component C-4 at BE of 290.4 eV can be assigned either to the presence O-C=O [23] or aromatic C=C π bonds (π - π * transition)[26]. The obtained intensity ratio between these four component spectra is (C-1: C-2: C-3: C-4 = 1: 0.2: 0.12: 0.21). The C 1s spectra obtained from the Pt loaded CNPs/Pt sample shown in Fig. 1c also comprises of these four species with a relative intensity ratio of 1: 0.33: 0.16: 0.12 between the components C-1, C-2, C-3 and C-4. The N 1s spectrum obtained from the CNP sample is weak and broad. In order to keep the analysis meaningful, we have decomposed the N 1s spectra with minimum number of component spectrum. The spectral decomposition shows presence of two components having BE's of 400.9 eV and 402.6 eV. The lower BE component was assigned to the presence of C=N bonds [27,28] whereas the higher BE component might be coming from N=O [27] or protonated –NH_2 [27] kinds of species. The estimated number density ratio between N and C in the CNP sample is around 2.4%. Pt 4f XPS spectra collected from the Pt loaded CNPs/Pt sample is shown in Fig 1d. The decomposition of the Pt 4f spectra shows presence of three types of Pt species. The higher intensity components having Spin-Orbit split BEs of 71.4 eV and 74.8 eV suggests predominant presence of metallic Pt (0) states [25,26]. The other two higher BE components (Pt-2 and Pt-3) are associated with the presence of Pt(II)O and Pt(IV)O_2 species in the sample[25,26]. The number ratio between loaded Pt with respect to C is 1.2%, obtained from the analysis of the area of the photoemission signal. The morphology of the photocatalyst was observed through Transmission Electron Microscopy (TEM). The TEM micrographs of CNPs (Fig.3) show the presence of clusters of aggregated carbon nano particles. It also shows that fusion and interconnection of primary particles takes place, giving rise to agglomerates. The carbon nano particles are in the form of elongated spherules. Fig.4. shows TEM micrographs of CNPs/Pt. It can be clearly seen that the Pt particles are homogeneously dispersed on the external surface of CNP owing to their photodeposition.

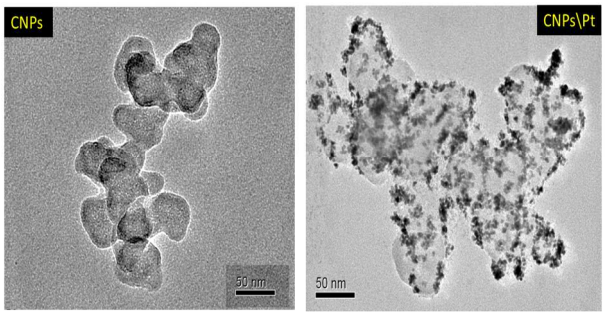

Fig.2 Transmitted electron micrographs of the as synthesized CNPs and Pt loaded CNPs/Pt sample.

Elemental Analysis of the CNPs revealed that they mainly contain elemental carbon C= 91. 95%, H = 0.053%, N= 0.045 % and S=0%.

The UV-DRS spectrum of CNPs/Pt reveals broadband absorption from 300-700 nm (Fig.5). The broadband absorption observed in addition to the absorption of CNP in UV region at about 340 nm makes it a promising material capable of exploiting the solar radiation from UV-NIR region.

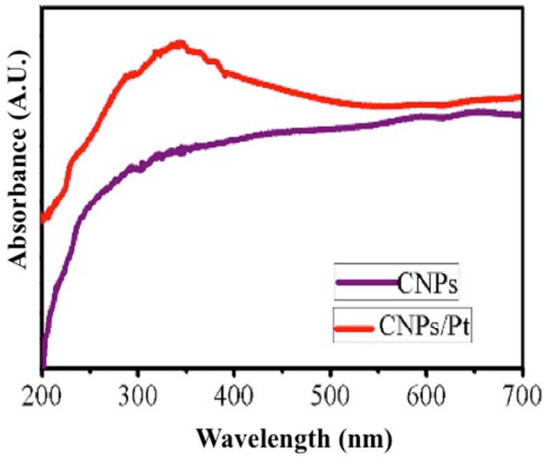

Fig.5 UV-DRS spectra of CNPs/Pt

Photodeposition of Pt

Photodeposition of PtNPs on CNPs is a pivotal step in the formation of platinized carbon nanostructured composites (CNPs/Pt). It therefore, becomes imperative to monitor the deposition of these Pt NPs as a function of time. To study this aspect, experiments were carried out wherein, a known amount of CNPs was taken in water and to them Pt and ethanol were added. These were then irradiated with light for different time intervals. Table 1. summarises the photodeposition of Pt as a function of time.

Table 1. Photodeposition of PtNPs on CNPs as a function of time

S.No	Time (min)	% Deposition of Pt
1.	15	95.1
2.	30	98.9
3.	45	99.1
4.	60	99.4
5.	120	99.9

It is evident that, nearly 99% of $PtCl_4^-$ ions get photoreduced in the form of PtNPs within 45 minutes of its exposure to light. The formation of platinum nanoparticles in the presence of ethanol and water takes place through a series of steps as reported earlier by Harada *et al.*[29] Initially, reduction of $PtCl_6^-$ ion to $PtCl_4^{-\cdot}$ which is relatively a fast process, takes place under photo irradiation.

$$PtCl_6^{2-} + RCH_2OH + h\nu \longrightarrow PtCl_6^{3-} + RCH_2O + H^+$$

$$PtCl_6^{3-} \longrightarrow PtCl_5^{2-} + Cl^-$$

$$PtCl_5^{2-} + {}^{\cdot}RCH_2O \longrightarrow PtCl_4^{2-} + RCH{=}O + HCl$$

$$PtCl_5^{2-} \longrightarrow PtCl_6^{2-} + PtCl_4^{2-}$$

Further reduction of $PtCl_4^{2-}$ to Pt in zerovalent state is relatively a slow process, achieved in two steps. In the first step, Cl dissociates from $PtCl_4^{2-}$, followed by the reduction of Pt^{2+} to Pt^0.

Optimization of reaction parameters

There are several parameters that can influence the photocatalytic hydrogen yield like photocatalyst dose, illumination intensity, irradiation time, presence and type of sacrificial donor etc. and therefore it is of utmost importance to study the effect of these parameters and optimize them for achieving the maximum hydrogen yield. The effect of these parameters was studied through offline evaluations mentioned earlier and discussed in detail below.

Photocatalyst dose

The amount of photocatalyst used in photocatalytic reaction is one of the important parameters as it directly influences the hydrogen yield. The amount of CNPs was varied in the range of 0.01 mg-0.06 mg/10 mL (Fig.6) of water keeping all the other experimental conditions constant. The highest hydrogen yield of 7525 mmol $h^{-1}g^{-1}$ (hydrogen evolution rate of 150.5 µmol h^{-1}) of photocatalyst was observed at a photocatalyst dose of 0.02 mg/10 mL of water. At lower photocatalytic dose the hydrogen yield could be lower due to less number of active sites whereas with an increase in the photo catalytic dose there is a decrease in the optical path length. This reduction in the effective intensity of photons leads to a decrease in photogenerated electrons and holes, consequently leading to a decreased activity at higher doses.

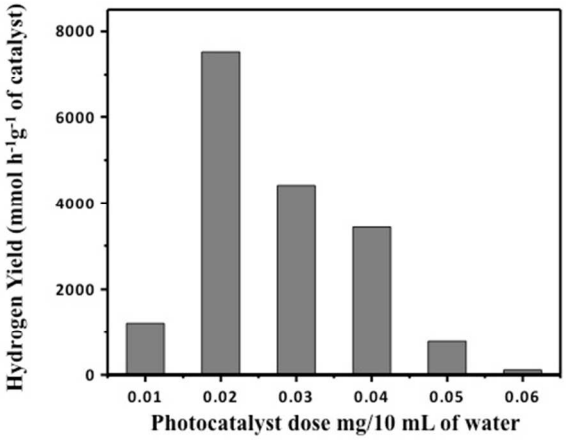

Fig. 6 Effect of photo catalyst dose on hydrogen generation by CNPs/Pt (Time: 2h, Illumination: 200W×2 tungsten lamps, Water: Ethanol – 20:1

Illumination Intensity

In a photocatalytic reaction, the amount of irradiated photon catalyses the reaction and hence the photocatalytic activity strongly depends on it. The illumination intensity was varied, by varying the wattages of tungsten filament lamps (100 W, 200 W and 400 W). It was observed that with the increase in illumination intensity the hydrogen yield increased (Fig.7).

The significant increase in the hydrogen evolution rate may be attributed to several factors. External illumination with 400W leads to heating of the system, which facilitates hydrogen generation. A temperature of 80 ^{o}C has been observed. This enhanced rate cannot be related to induced reaction steps only, but can be rationalized in terms of following considerations:

1. With an increase in the temperature, the solubility of oxygen decreases.
2. More facile desorption of intermediate species adsorbed on surface.
3. Acceleration of "Dark" catalytic reaction on the surface of the catalyst.

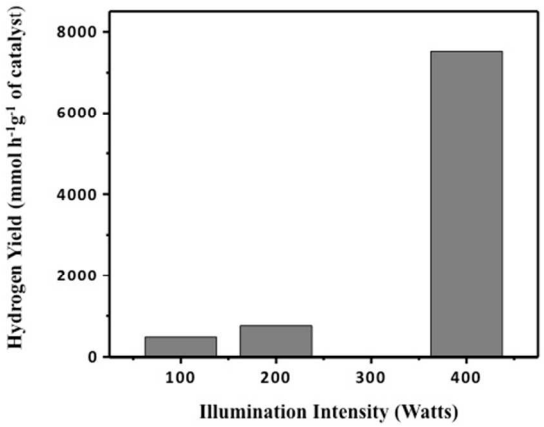

Fig.7 Effect of Illumination intensity on hydrogen generation by CNPs/Pt. (Photocatalyst dose=0.02mg/10mL, Time: 2h, Water: Ethanol – 20:1)

The last factor can contribute significantly through reaction between photogenerated oxygen adsorbed on the surface of CNP with sacrificial donor employed like ethanol and other intermediates. The increased temperature probably leads to higher reaction rates between photogenerated oxygen (holes, super oxides, intermediate oxidants) and sacrificial donor with the consequent increase in the photoinduced hydrogen production.

Sacrificial Donor

Water splitting is an uphill reaction and not thermodynamically favourable. Moreover, the recombination of photogenerated electrons and holes further affect the photo catalytic efficiency. Sacrificial donors are generally added which act as hole scavengers thereby preventing the recombination reaction and thereby increasing the photocatalytic activity. The effect of the sacrificial donor was studied by varying the sacrificial donors. Highest hydrogen yield was obtained where ethanol was used as the sacrificial donor followed by mono ethanolamine and methanol as shown in Fig.8. In case of alcohol-water mixtures, it is reported that the interaction of valence band holes with alcohol and water lead to formation of H^+ leading to an increased hydrogen yield as per the following reactions [30]:

$$2h^+ + H_2O \longrightarrow 2H^+ + ½\ O_2 \text{ or } H^+ + {}^{\cdot}OH$$

$$2h+ + C_2H_5OH \longrightarrow 2H^+ + CH_3CHO$$

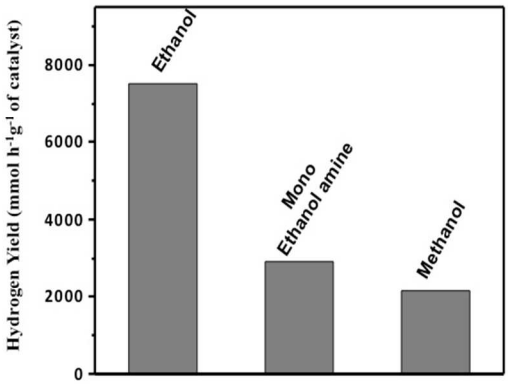

Fig.8 Effect of varying the sacrificial donor (Photocatalyst dose=0.02mg/10mL, Time: 2h, Illumination: 200W×2 tungsten lamps, Water: Ethanol – 20:1)

As a result of these interactions, the intermediates (acetaldehyde) that are consequently formed may further lead to the formation of protons, which are finally reduced to hydrogen at the reduction site of the metal.

Comparison of CNPs, Pt NPs and CNPs/Pt

To illustrate the role of the each of components of the synthesized photocatalyst and to understand the underlying mechanism, we compared the photocatalytic activity of each of the involved components individually as well as in combination with each other. An identical set of experiments was carried out using only CNPs, only PtNPs, admixture of PtNPs and CNPs and platinized carbon nanostructured composites. The results were as shown in Fig. 9.

The enhanced activity of the platinized carbon nanostructured composite is attributed to the Surface Plasmon Resonance (SPR) effect of the platinum nanoparticles photodeposited on the surface of CNPs. There are three independent energy transfer processes that govern the SPR effect, thereby increasing the concentration of charge carriers. These are SPR mediated charge transfer from the metal to the semiconductor, near field electromagnetic radiations and scattering mechanism [31]. It is known that if the involved components, in this case, the metal nanostructures (PtNPs) and the semiconductor (CNPs) are in close proximity with each other, then all the three mechanisms play a role in enhancing the photocatalytic activity. However, if some distance separates them, then only near field electromagnetic and scattering mechanism maybe the reason behind the improved activity. Also, with an increasing distance from the surface, the effect may significantly decrease. The above results are a clear indication of these facts.

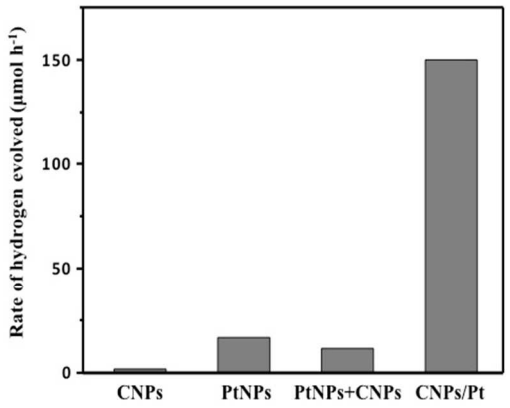

Fig.9 Comparison of CNPs, Pt NPs and CNPs/Pt

In case of PtNPs +CNPs admixture, where first the PtNPs were formed and then mixed with CNPs, both the nanoparticles are not in close contact with each. However, in case of CNPs/Pt, the PtNPs get photo deposited onto the CNPs and hence are in close proximity. This facilitates effective charge transfer between them and also helps in concentration of these charge carriers through scattering and near field electromagnetic radiation mechanisms. As far as the significantly lower activity of individual components are concerned (CNPs & PtNPs), several studies have already proven that the composites exhibit higher photo activity as compared to their pure counterparts.

Photocatalytic activity

The photocatalytic activity of the platinized carbon nanostructured composite was evaluated for hydrogen production under UV-Vis irradiation (Fig 10).

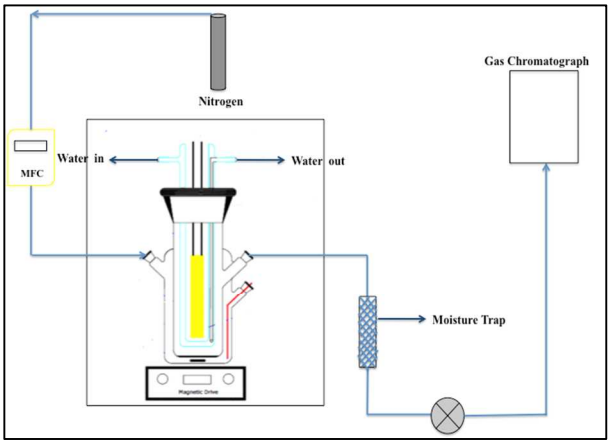

Fig.10: Experimental setup for online photo catalytic evaluations

A steady hydrogen evolution rate of 20 μmol h^{-1} was observed as the reaction progressed for 24 h. Fig.11 shows the time dependency of hydrogen evolution observed. It is evident that there is a steady increase in the hydrogen evolution with time and no apparent decline was observed up to 24 h. The total amount of hydrogen that was produced after 24h was 0.44 mmol (9.856 mL). The stability of the catalysts was also monitored in a separate experiment and the photocatalyst showed stability up to 70 h, which is quite significant in terms of solar hydrogen production.

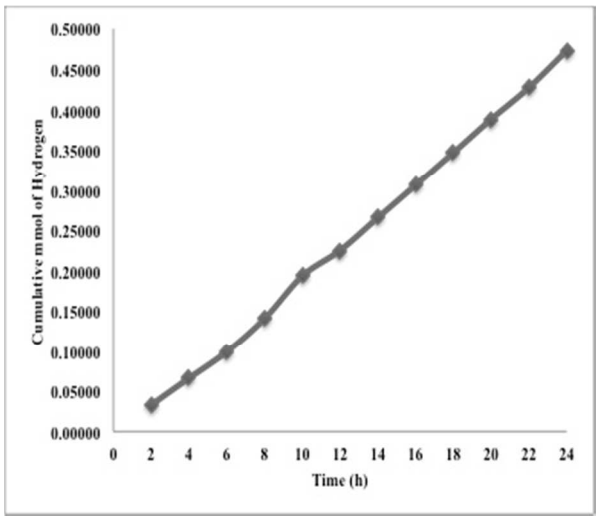

Fig.11 Hydrogen evolution by CNPs/Pt as a function of time

Photothermal Activity vs Photocatalytic activity

A marked difference was observed in the hydrogen evolution rate in case of offline and online evaluations. There are a number of factors that may contribute to this. Apart from the difference in the reactor configuration and reaction volume, the obvious difference lies in the source of illumination and temperature. While in case of vials, the illumination source is a tungsten filament lamp, which constitutes 85 % of IR radiation and 15-20% of visible radiation and 1% of UV radiation; the high-pressure mercury lamp has 45% visible radiation. There is also a difference in the reaction temperature between the two cases. In case of vials, the temperature is in the range of 70-80 ^{o}C, while in case of inner radiation cell; the temperature is maintained close to ambient (20^{o}C). However, it needs to be borne in mind that despite the temperature remaining close to ambient, the photo catalytic activity is reasonably good (20 μmol h^{-1}). This maybe tied to the SPR effect of PtNPs and carbon nanostructures thereby facilitating localized heating which compensates well for the temperature maintained at 20 ^{o}C. It is possible, that since carbon is known to be a good absorber, it absorbs IR radiations significantly which may lead to rise in temperature in case of vials. In addition to this, the localized heating aids in enhancing the hydrogen evolution rate by virtue of the thermal effect as discussed earlier under effect of illumination intensity. To substantiate the effect of localized heating, a simple experiment of evaporation of water by CNP, CNPs/Pt and PtNPs under solar light was carried out, wherein CNPs/Pt showed the highest evaporation of water illustrating the influence of localized heating as reported by others as well for different nanoparticles [32]. Efforts were undertaken to replicate the system with photothermal conditions similar to that observed in case of borosilicate vials (offline evaluations), however, the present system showed hydrogen evolution rate which was significantly lower which was ascribed to the volatilization of the sacrificial donor (ethanol). It is also envisaged to design reactor wherein the increase in the temperature can be monitored independent of the pre-set temperature of 20 ^{o}C presently required in the system due to the use of mercury vapour lamp.

Plausible Mechanism

Pt, which is deposited on the surface of CNPs during the course of photocatalytic reaction enhances the photocatalytic activity by acting as a co-catalyst as well as due to the SPR effect exhibited by it.

Typical steps taking place during the reaction are as follows:

1. On illumination of CNPs with a light source, there is a charge separation leading to the formation of photogenerated electrons and holes. The electron migrates to the conduction band leaving the hole in the valence band.

2. As the Fermi energy levels of Pt are more negative than the conduction band potential of CNPs, transition of conduction band electron from CNPs to Pt takes place.

3. Pt, which was added along with the catalyst, is photo deposited on the surface of CNPs by the electrons present in the conduction band of CNP.

4. Ethanol added as the sacrificial donor helps in suppressing the recombination reaction by quenching the holes.

5. The protons on the surface of Pt are finally reduced to hydrogen. Pt is involved in different energy transfer mechanisms, which significantly enhances the photocatalytic activity.

Efforts are being made to illustrate the SPR effect of Pt in enhancing the photocatalytic activity of CNPs. The possible rationalization could be as follows: Pt acts as a sensitizer and absorbs the light in the UV-Vis range. However, due to the energetically unfavourable condition,

the electrons generated are not transferred leading to localized heating. This may lead to increased charge formation with consequent increase in photo catalytic activity. Also, two other energy transfer mechanism which probably play a role are as following: i) Interaction of CNPs with the strong electric fields generated by the Pt due to SPR. Due to these intense electric fields, the number of photogenerated electrons and holes increases and ii) Scattering of photons by plasmonic Pt helps in increasing the effective photon path length, in turn increasing the number of photogenerated electrons and holes These two effects probably increase the hydrogen evolution rate.

Conclusions

In summary, platinized carbon nanostructured composites were successfully prepared by combustion of a hydrocarbon precursor followed by photodeposition of platinum nanoparticles on carbon nanostructures. The CNP matrix helps in efficient dispersion of platinum nanoparticles and this proximity of Pt NPs with CNPs aids in enhancing the photo catalytic activity through the SPR effect. Temperature has a pronounced effect on the photo activity of platinized carbon nanostructured composites. A steady hydrogen rate of 20 µmol h^{-1}, aqueous stability as well as inexpensive nature of carbon make this photocatalyst promising.

Acknowledgements

The authors would sincerely like to acknowledge CSIR-Network Project (NWP-56) for financial assistance. The authors would also like to thank Dr. Manaswita Nag for providing assistance during TEM analysis at Indian Institute of Science, Bangalore.

Notes and references

[a] CSIR-Network Institute of Solar Energy (CSIR-NISE), India.
[b] Environmental Materials Division, CSIR-NEERI, Nehru Marg, Nagpur-440020
[c] Solid State and Structural Chemistry Unit, Indian Institute Science, Bangalore, 560012.

† Footnotes should appear here. These might include comments relevant to but not central to the matter under discussion, limited experimental and spectral data, and crystallographic data.

Electronic Supplementary Information (ESI) available: [details of any supplementary information available should be included here]. See DOI: 10.1039/b000000x/

1 H. Yoon, S. Ko and J. Jang, *Chem. Commun*, 2007, 1468.
2 F. Rodríguez-reinoso, *Carbon*, 1998, **36(3)**, 159.
3 H. Wang, A. Keller and F. Li, *J. Environ. Eng*, 2010, **135 (10)**, 1075.
4 X. Rex, C. Chena, M. Nagatsu and X. Wang, *Chemical Engineering Journal*, 2011, **170**, 395.
5 B. Gao, C. Bower, J. Lorentzen, L. Fleming, A. Kleinhammes, X.Tang, L.M cNeil, Y. Wu and O. Zhou, *Chem. Phys. Lett.*, 2000, **327**, 69.
6 C.W. Zhou, J. Kong and H.J. Dai, *Appl. Phys. Lett.*, 2000, **76**, 1597.
7 J. Lee, *Appl. Phys. Lett.*, 2005, **87**, 3.
8 D. Vairavapandian, P. Vichchulada, M. Lay, *Analytica Chemica Acta*, 2008, **626**, 119.
9 N. Sinha, J. Ma, and J. T. W. Yeow, *J. Nanosci. Nanotechnol*, 2006, **6(3),** 573**.**
10 H. Kroto, J. Heath, S. O'Brien, R.Curl and R. Smalley, *Nature*, 1985, **318**, 162.
11 S. Iijima, *Nature*, 1991, **354**, 56.
12 H. Liu, T. Ye and C. Mao, *Angew. Chem.*, 2007, **46**, 6473.
13 K. Dai, T. Peng, D. Ke and B. Wei, *Nanotechnology*, 2009, **20,** 125603.
14 J. Zhang, X. Zhao, S.Kang, P. Yao, X. Li and J. Mu, *Advanced Materials Research,* 2011, **239-242,** 1686.
15 Q. Li, B. Guo, J. Yu, J. Ran, B, Zhang, H. Yan, and J. Gong, *J. Am. Chem. Soc*, 2011, **133,** 10878.
16 X. Wang, K. Maeda, A. Thomas, K. Takanabe, G. Xin, J. Carlsson, K. Domen, and M. Antoinietti, *Nat. Materials*, 2009, **8**, 76.
17 B. Chai, T. Peng, P. Zeng and X. Zhang, *Dalton Trans*, 2012, **41**, 1179
18 A. Ye, W. Fan, Q. Zhang, W. Deng and Y. Wang, *Catal. Sci. Technol*, 2012, **2**, 969.
19 A. Suryavanshi, P. Dhanasekaran, D. Mhamane, S. Kelkar, S. Patil, N. Gupta and S. Ogale, *Int. J. Hyd. Energy, 2012,* **37(12),** 9584.
20 I.Akimoto, K.Maeda and N. Ozaki, *J. Phys. Chem. C*, 2013, **117,** 18281.
21 E.Graham, C. Macneill and N. Levi-Polyachenko, *NanoLIFE* 2000, **35**, 3523.
22 P.Kamat, *The Electrochemical Interface*, 2006 **15 (1),** 45**.**
23 S.C. Ray, A.Saha, N.R. Jana and R. Sarkar, *J. Phys. Chem C,* 2009, **113**, 18546.
24 D. Solomon, J. Lehmann, J.Wang, J. Kinyangi, K. Heymann, Y. Lu, S.Wirick and C. Jacobsen, *Sci. Tot. Env,* 2012, **438**, 372.
25 A.K. Shukla, A.Hamnett, A.Roy, S.R. Barman, D.D. Sarma, V.Alderucci, L.Pino nd N. Giordano, *J.Electroanal.Chem* , 1993, **352**, 337.
26 A.S. Aricò, V. Antonucci, N. Giordano, A.K. Shukla, M.K. Ravikumar, A.Roy, S.R. Barman and D.D. Sarma, *J. Power Sources*, 1995, **50**, 295.
27 A.P. Dementjev, A. de Graaf, M. C. M. van de Sanden, K. I. Maslakov, A. V. Naumkin, A. A. Serov, *Dimond and Related Materials,* 2000, **9**, 1904.
28 F. Rossi, B. Andre, A. van Veen, P. E. Mijnarends, H. Schut, F. Labohm, H. Dunlop, M. P. Delplancke, K. Hubbard, *J. Mater. Res.,* 1994, **9**, 2440.
29 M. Harada and H. Einaga, *Langmuir*, 2006, **22**, 2371.
30 A. Patsoura, D. I. Kondarides and X.E. Verykios, *Appl. Catal., B*, 2006, **64**, 171.

31 S. Linic, P.Christopher and D. Ingram, *Nature Materials*, 2011, **10**, 911.
32 O. Neumann, A.Urban, J. Day, S. Lal, P. Nordlander, N.J. Halas, *ACS nano*, 2013, **7 (1)**, 42.